Research paper

Stress state of reinforced concrete walls of grain silos subjected to static and thermal actions – in situ tests and numerical analysis

Jolanta Anna Prusiel[1], Andrzej Marynowicz[2]

Abstract: In used reinforced concrete grain silos, failures occur (e.g., increased cracking of reinforced concrete walls). These failures may be caused by overloading of the chamber structure due to a sudden drop in ambient temperature throughout the day. These daily drops in ambient temperature cause thermal stresses in the silo shell. Additional thermal stresses in the silo are caused by the interaction of the wall and the bulk material stored within the silo. This results in additional tensile stresses in the cross-sections of the silo chamber wall, combined with bending. This paper presents the results of in situ studies of early winter temperature field distributions in a grain elevator at the Podlaskie Grain Plant in Białystok. A specialized prototype SensoNet telemetry system was used for the on-site tests, enabling continuous monitoring of operating silo batteries and recording physical quantities such as deformation and temperature. The measured variable temperature fields on the surface of the silo chambers were used to determine nonlinear temperature distributions across the thickness of the reinforced concrete walls in the grain silo battery using the finite difference method. Numerical calculations of four interlocking grain silos subjected to static (Janssen pressure of bulk material) and thermal loads were performed using the finite element method. Analysis of the numerical calculation results (FEM) demonstrates the unfavorable effects of thermal and static load coupling in the form of increases in latitudinal tensile stresses and bending moments in the reinforced concrete walls of the grain silo batteries.

Keywords: numerical analysis, grain silo, reinforced concrete wall, stress state, thermal action

[1]DSc., PhD., Eng., Bialystok University of Technology, Faculty of Civil Engineering and Environmental Sciences, ul. Wiejska 45E, 15-351 Bialystok, Poland, e-mail: j.prusiel@pb.edu.pl, ORCID: 0000-0001-6827-1059

[2]DSc., PhD., Eng., Opole University of Technology, Faculty of Civil Engineering and Architecture, ul. Katowicka 48, 45-061 Opole, Poland, e-mail: a.marynowicz@po.edu.pl, ORCID: 0000-0002-8308-8479

1. Introduction

Silo structures are objects with a higher degree of risk and threat of disaster, compared to other engineering structures. The most common causes of emergency situations and silo disasters include: errors in the structural design and construction (errors in design procedures, underestimated loads, insufficient structural reinforcement (Fig. 1b), low quality concrete), operation of the silo inconsistent with the design assumptions, e.g. too high a speed of silo emptying, material fatigue caused by the dynamic nature of interactions in the silos, low-cycle fatigue of the silo structure [1–4]. Furthermore, there is a risk of spontaneous combustion and dust explosions in silos when storing bulk media susceptible to dust explosions, which include, among others, cereals [5].

(a)   (b)
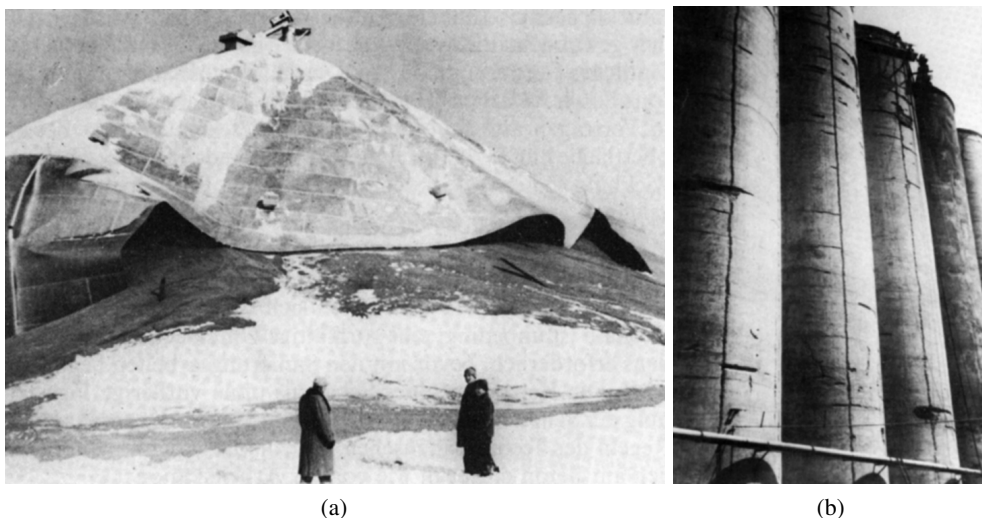
Fig. 1. (a) Construction disaster of a steel silo in winter in St. Joseph, Missouri (USA), (b) View of vertical cracks in the reinforced concrete walls of the silo (pre-failure state, USA) [1]

According to the standard [6], reinforced concrete silo structures are designed for a service life of at least 100 years (structure class S6). Therefore, these facilities should be monitored and inspected for their technical condition during long-term operation to ensure their reliability and durability [7–9]. In order to ensure the appropriate level of reliability and durability of silo structures at the design stage, the standard [10] introduced appropriately differentiated procedures for determining loads from bulk medium pressure, depending on the action assessment class to which the silo was classified (Table 1). Thus, for silos with a large storage mass and silos emptied or filled at large eccentricities (class AAC3), the procedure for calculating actions was expanded. In these silos it is also recommended to experimentally determine the properties of the bulk material according to Annex C in [10], which significantly increases the cost of designing the silo.

Table 1. Classification of impact assessment on silo according to the standard [10]

Action Assessment Class	Class characteristics
Class 3 (AAC3)	Silos with capacity in excess of 10 000 tonnes Silos with capacity in excess of 1000 tonnes in which any of the following design situations occur: a) eccentric discharge with e_0/d_c >0.25, b) squat silos with top surface eccentricity with e_t/d_c >0.25, where: e_0 – chamber discharge eccentricity, e_t – chamber filling eccentricity, d_c – internal diameter of the chamber.
Class 2 (AAC2)	All silos covered by PN-EN 1991-4 [10] and not placed in another class.
Class 1 (AAC1)	Silos with capacity below 100 tonnes.

Complex deformation and stress states in the cross-sections of chamber and hopper structures, resulting from randomly varying interactions of bulk media combined with non-stationary temperature fields, can also lead to silo failure. Additional thermal stresses (tensile stresses) combined with bending occur, causing increased cracking of the reinforced concrete walls (Fig. 1b). In grain silos, pressure changes on the silo walls are also observed during initiation and material flow in the silo chamber [11], and local pressure increases may also occur at the connection between the wall and the hopper [12].

A spectacular silo failure on a bulk medium, after which research began on taking into account ambient temperature drops in silo loads, was the failure of a steel silo in St. Joseph, Missouri (USA) in the winter of 1962/1963, with the temperature dropping to −23°C (Fig. 1a). In this region, the maximum temperature in summer was +40°C, and in winter it dropped to −40°C [1]. As a result of the analysis of the causes of the steel silo failure and the results of research by, among others, Anderson [13] and Theimer [14], it was found that daily drops in the ambient temperature of silo walls in early winter and spring cause thermal stresses, which result in additional bending and stretching of the silo wall. The occurrence of additional thermal stresses in the silo is caused by the interaction of the wall and the bulk medium. In a chamber filled with a bulk medium (e.g., grain), a drop in temperature causes a shortening of the shell circumference, which is limited by the flexibility of the core of the stored granular material. This effect results in an increase in the horizontal component of the bulk medium pressure and the occurrence of significant thermal stresses, causing stretching in the cross-sections of the silo shell combined with bending. Stress tests of the operating chambers of the PZZ grain elevator in Białystok during winter and spring revealed an increase in tensile stresses in the wall reinforcement by several MPa in the chamber's zone of strong sunlight [15]. This issue was also analysed in a selected research works [16–22].

The unfavorable effects of the coupling of static and thermal actions in reinforced concrete walls of free-standing grain silos can be determined in a simplified manner (in a plane stress state) based on the standards [10,23]. In accordance with the applicable European standard [10],

the additional normal component of the pressure on the cylindrical silo wall caused by a drop in ambient temperature in a short time can be calculated from the formula

$$(1.1) \qquad p_{hT} = C_T \alpha_w \Delta T \frac{E_w}{\left[\dfrac{r}{t} + (1 - \nu) \dfrac{E_w}{E_{sU}} \right]}$$

where: C_T – temperature load factor, α_w – coefficient of thermal expansion of the silo wall, ΔT – temperature drop across the thickness of the silo wall, r – silo chamber radius, t – silo chamber thickness, E_w – elastic modulus of the silo wall, ν – Poisson's ratio of the particulate solid, $\nu = 0.3$ acc to [10], E_{sU} – the unloading effective elastic modulus of the stored solid according to Annex C.10 in [10].

The national standard [23], replaced by Eurocode [10], proposed to calculate the additional latitudinal tensile force in a flat ring cut out of the shell cooperating with the bulk medium from the relationship

$$(1.2) \qquad N_\theta^T = \frac{0,5 d_c E_m \alpha_t \Delta T_{sr}}{\dfrac{0,5 d_c E_m}{t E_c} + (1 - \nu_m)}$$

where: ΔT_{sr} – daily average temperature drop across the thickness of the silo wall, d_c – silo chamber diameter, t – silo chamber wall thickness, E_c – elastic modulus of the concrete, E_m – elastic modulus of the bulk medium, determined analytically according to [23], ν_m – Poisson's ratio of the bulk medium, $\nu_m = 0.4$ according to [23].

Also in a simplified way, assuming a linear-elastic stress state in the reinforced concrete silo wall, the latitudinal bending moment caused by the temperature difference across the chamber thickness can be determined as [24]

$$(1.3) \qquad M_\theta^T = \frac{\alpha_w \Delta T E_c J_c}{t}$$

where: ΔT – temperature drop across the wall thickness, E_c and J_c – elastic modulus and moment of inertia of the concrete wall cross-section, respectively, t – silo chamber wall thickness.

However, in the case of a battery of grain silos, a spatial computational model using the finite element method should be used to analyse the effects of coupling the static pressure of the bulk material and daily temperature drops [21, 22, 25–27]. This paper presents, based on the results of numerical analysis, the stress state of reinforced concrete walls in a battery of four grain silos subjected to static and thermal effects in a three-dimensional problem. The computational model of the interlocking chambers used in the FEM analysis was extended compared to the model used in [21, 22, 25] by modelling the reinforced concrete wall using solid elements. The numerical analysis utilized the results of in situ tests in the form of non-stationary temperature fields measured on the surface of the concrete silo wall during the winter season using a telemetric system.

2. Thermal actions in the silo chamber

2.1. In-situ studies of silo chamber

Stress tests of reinforced concrete walls of a battery of grain silos subjected to ambient temperature drops were carried out on an operating elevator of the Podlaskie Grain Plant in Białystok (Fig. 2), as part of a research project carried out in 2001–2003 by a team of researchers from the Bialystok University of Technology [15]. The aim of the tests was to determine the redistribution of tensile stresses in the latitudinal reinforcement of the silo chambers and to determine the corresponding daily temperature drops on the wall surface. The battery of reinforced concrete grain silos was built in the 1970s. Two chambers with the following characteristics were selected for the study: height 29.5 m, internal diameter 8 m, and wall thickness 0.20 m. Measurement points on the circumference of one chamber were placed at a height of 6 m, 8 m, and 10 m above ground level, and at a height of 8 m in the other chamber (Fig. 2b). Both chambers were filled with grain during the study (phase after filling).
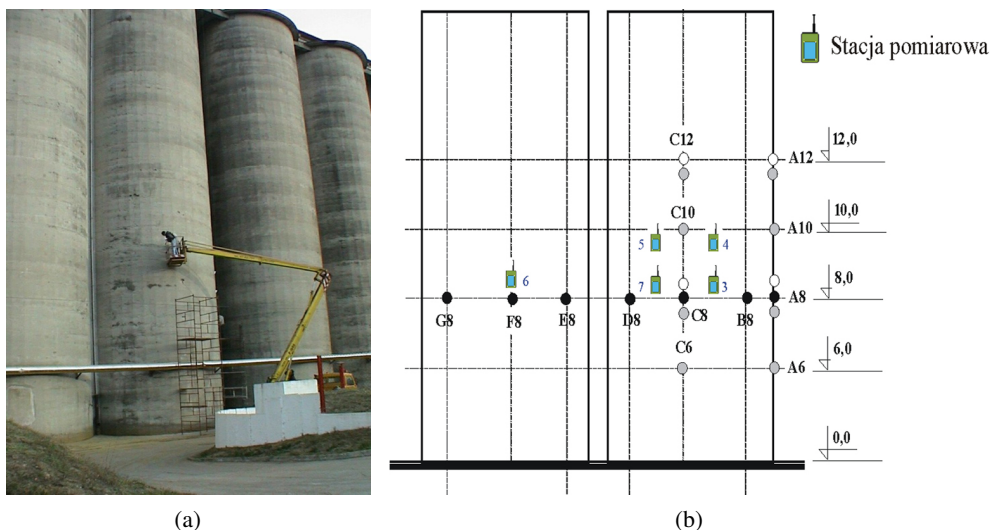

Fig. 2. The battery of cylindrical grain silos: (a) preparation of the silo chambers for testing, (b) diagram of the measurement point layout

In situ tests were conducted in multi-day cycles during winter (December 2002) and spring (March–April 2003). A specially designed SensoNet telemetry measurement system was used for the tests, enabling long-term monitoring of deformation in the perimeter reinforcement combined with measurement of temperature fields on the concrete wall surface and reinforcement [28]. The prototype SensoNet measurement system used radio transmission to collect data from measurement points located on a battery of silos (Fig. 2b). Measuring and transmitting stations (telemetry modules) were placed on the surface of the tested silos, recording readings from selected strain gauges and temperature sensors in their own memory.

The results were periodically transmitted to the main station connected to a portable computer equipped with software for recording data from the facility. The results obtained from the tests of the PZZ grain silos battery in Białystok using the SensoNet telemetric measurement system are described in more detail in the works [15, 28, 29].

Selected results from in situ tests needed for further analysis of stress states of reinforced concrete walls of silo batteries subjected to variable thermal impacts are presented in Fig. 3 and Table 2. Figure 3 shows non-stationary distributions of temperature fields read in a 7-day cycle in the winter period (from 07.12.2002, 13:30 to 14.12.2002, 12:30) on the surface of the concrete silo wall, at selected measurement points in the zone of strong insolation (points E and F) and in the shadow zone (points B and G) at a height of 8 m above the ground level. The period of the greatest daily temperature drops of the wall was 19 hours, for which the temperature values were read from the graphs and presented in Table 2. The maximum daily temperature drops on the wall surface were used to calculate non-linear temperature distributions on the thickness of the silo wall at points B, E, F, G using the finite difference method.
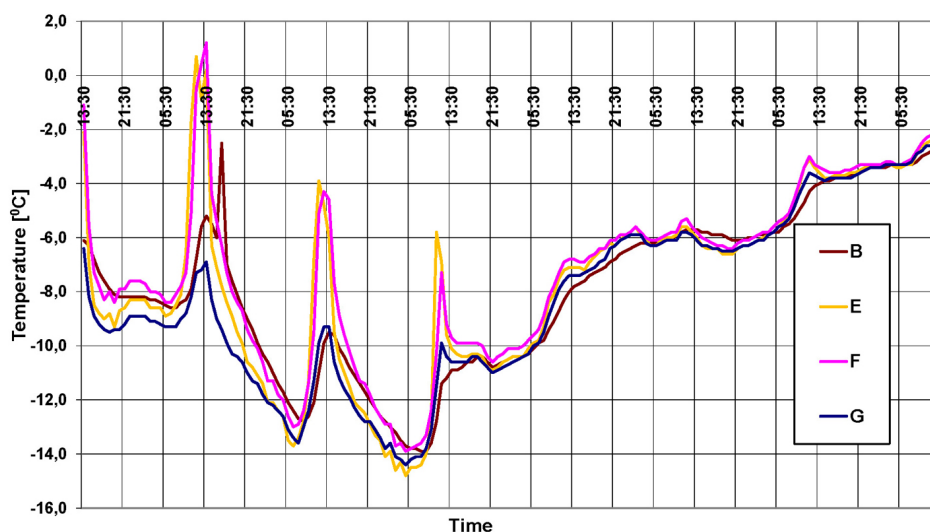

Fig. 3. Temperature field distributions on the surface of reinforced concrete chambers of the silo battery in Bialystok measured at points B, E, F and G in winter (December 2002)

Table 2. Maximum daily temperature drops on the surface of the silo battery wall (December 2002)

Temperature		Measurement points			
[°]		B	E	F	G
13:30	T_0	−5.2	+0.2	+1.2	−6.9
8:30	T_k	−12.8	−12.8	−12.4	−13.0
$\Delta T = T_k - T_0$		−7.6	−13.0	−13.6	−6.1

2.2. Temperature field distributions in the silo wall

Theoretical temperature field distributions across the wall thickness of a silo filled with wheat were calculated using a computer program using the finite difference method. The program allows for the calculation of temperature and humidity field distributions in cylindrical reinforced concrete silos under stationary conditions (constant ambient temperature and humidity) and unsteady heat and moisture flow conditions (time-varying ambient temperature and humidity).

The problem of unsteady heat and moisture flow in a cylindrical silo chamber and a granular medium was limited to an axisymmetric problem. The reinforced concrete partition (silo wall) and the bulk medium filling it were modeled as a set of circular surfaces with a common axis (2D model). Unidirectional heat flow and moisture transport were assumed, meaning that temperature and humidity change only in the radial direction. The theoretical assumptions of the heat flow and moisture transport model in the reinforced concrete silo chamber and the bulk medium stored within utilized fundamental relationships arising from the technical theory of unsteady heat flow in contact problems of solids, as well as known laws of physics describing the mechanisms of moisture transport in capillary-porous materials, taking into account the physical properties of the materials [30–32]. The assumptions of the theoretical model of heat flow and moisture transport in cylindrical chambers of grain silos are presented in more detail in [25, 29].

Theoretical calculations of temperature distributions in the wall assumed non-stationary heat flow and constant environmental humidity (80%), due to the short time period (19 h) and small humidity changes in the silo environment. Theoretically calculated daily temperature drops ΔT_z on the external surface and ΔT_w on the internal surface of the silo chamber wall using the finite difference method (FDM) are presented in Table 3. The values ΔT_{avg} (average temperature drop in the wall) and ΔT (temperature gradient) were calculated from the linear temperature distribution across the wall thickness. The calculations show that significantly greater temperature drops occur in the sunlit zone (points E and F). On the external surface of the concrete wall exposed to sunlight, the wall temperature drop is 2.5 times greater than in the shaded zone of the silo chamber (points B and G).

Table 3. Theoretically calculated (FDM) temperature drops in the silo wall

Wall section	Point B	Point E	Point F	Point G
ΔT_z [°]	–4.9	–10.63	–11.09	–3.99
ΔT_w [°]	–0.87	–2.14	–1.81	–1.48
ΔT_{avg} [°]	–2.89	–6.39	–6.45	–2.74
ΔT [°]	–4.03	–8.49	–9.28	–2.51

Theoretically determined thermal interactions (Table 3) coupled with static load (pressure of bulk medium) were adopted for numerical analysis of stresses in reinforced concrete cylindrical walls of interlocking grain silos.

3. Numerical analysis

3.1. Computational model of a four-chamber silo

To analysis the stress states in reinforced concrete walls of grain silo batteries subjected to daily ambient temperature drops, a computational model of four cylindrical chambers connected monolithically was formulated, assuming interaction between the wall structure and the granular medium (Fig. 4, 5). The 0.20 m thick reinforced concrete silo wall was divided into 5 layers, and each layer was modeled using solid elements. The following shell discretization mesh was adopted: 150 horizontal strips with a height of 0.20 m along the shell generatrix and 60 vertical strips defined by the central angle (Fig. 4a, Table 4). In the numerical calculations, the shell was treated as fixed at its lower edge, while the upper edge was free to move. Numerical calculations of the silo batteries were performed using the ORCAN program, developed at the Bialystok University of Technology [33]. The program is based on the Finite Element Method and is used for static and dynamic calculations of building structures subjected to mechanical and thermal loads, in the scope of linear and non-linear analysis.
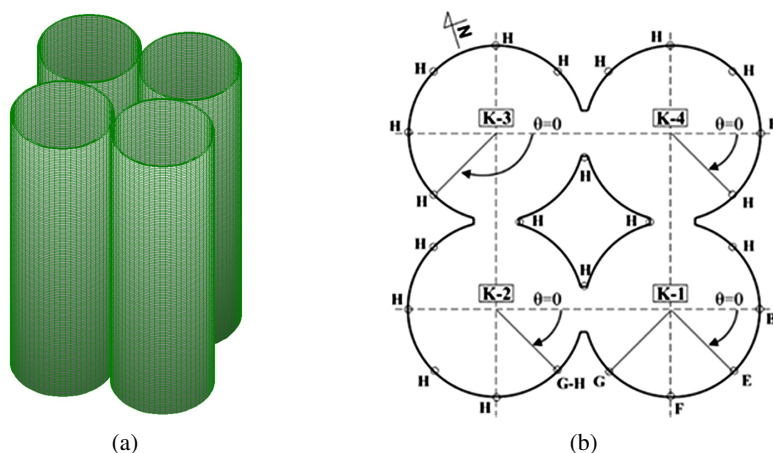

(a)   (b)

Fig. 4. Computational model of a battery of four chambers in the ORCAN program (FEM): (a) discretization grid of the interlocked chambers, (b) diagram of the arrangement of points B, E, F, G and H describing the distribution of the variable temperature on the wall surface

The static action in the form of pressure of the bulk material (wheat) on the silo chamber wall was determined based on the standard [10], using Janssen's theory, known for over a hundred years [34], used in the calculation of pressure in silos [24]. The physical and mechanical properties of wheat for determining the pressure of the bulk medium in the silo were adopted from Table E1, Annex E of the standard [10]. The calculated pressure of wheat in the phase after filling the silo is presented in Table 5. The pressure of the bulk medium in the silo chamber was modeled as axisymmetric, coupled with a non-stationary temperature field on the chamber surface, with values determined theoretically based on the results of in situ

Table 4. Discretization of the computational model of a four-chamber battery

Parameter	Four-chamber battery
Number of nodes in the model	249 584
Number of solid elements	178 220
Number of boundary elements	33 840
Total number of elements	212 060
Dimensions of the solid element (in the wall axis)	$l_1 = 0.429$ m; $h_1 = 0.20$ m; $t_1 = 0.04$ m

tests at the grain elevator in Białystok (Table 3). In the analysis of thermal interactions, it was assumed that chamber K-1 would be loaded with a variable temperature field on the perimeter (Fig. 4b). It was assumed that the remaining three chambers (K-2, K-3, and K-4) were located in the shadow zone and were loaded with a constant temperature drop on the wall surface (point H = G) along their entire perimeter. In the numerical calculations (FEM) of the battery of four chambers, a linear distribution of temperature drops across the wall thickness was assumed.

Table 5. Values of axisymmetric horizontal pressure p_{hf} in the silo chamber and horizontal deformations ε_h and the modulus of elasticity of wheat $E_{m,h}$

Depth from equivalent surface z [m]	Horizontal pressure after filling p_{hf} [kPa]	Horizontal deformation ε_h [–]	Elastic modulus $E_{m,h}$ [MPa]
1.0	5.02	0.0011	9.7
3.0	13.10	0.0018	16.4
5.0	19.12	0.0021	20.2
7.0	23.60	0.0023	22.7
10.0	28.28	0.0025	25.0
15.0	32.68	0.0027	27.1
20.0	34.78	0.0027	28.0
24.0	35.64	0.0028	28.4
25.0	35.79	0.0028	28.5
28.2	36.14	0.0028	28.6

Assuming a simple plane stress state, the interaction between the silo wall and the bulk medium (Fig. 5) was modeled using elastic constraints with the flexibility $C(z)$ given by the formula:

(3.1)
$$C(z) = \frac{E_m(z)}{R(1 - \nu_m)}$$

where: $E_m(z)$ – elastic modulus of the bulk material (wheat) at the depth of the chamber, ν_m – Poisson's ratio of the bulk material, R – silo chamber radius.
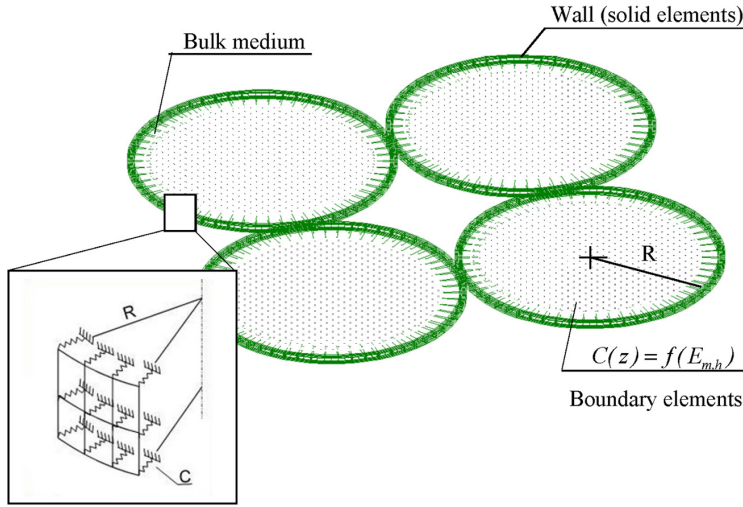
Fig. 5. Model of interaction between silo wall and bulk medium [29]

It is important to correctly determine the elastic modulus of wheat $E_m\,(z)$, which depends on the state of stress and strain in the bulk medium. To determine the flexibility of the bulk material in the discrete numerical model of the silo, functional relationships of stresses and strains in the bulk medium (formulas (3.2), (3.3)) are used, derived by Manbeck and Nelson [35] based on experimental tests of wheat in a triaxial compression apparatus. The elastic modulus of wheat in the horizontal direction, calculated on the basis of formulas (3.2), (3.3) and assumed in the numerical analysis, is given in Table 5.

$$(3.2) \qquad \varepsilon_h = 0.01(-4.92 + 12.20K - 4.71K^2)(p_{hf}/0.28)^{0.454}$$

$$(3.3) \qquad E_{m,h} = 2.203 \left(\frac{56,1}{-4.92 + 12.20K - 4.71K^2} \right)^{2.203} \varepsilon_h^{1.203}$$

where: p_{hf} – horizontal pressure on the silo wall after filling, given in MPa (Table 5), ε_h – deformation in the medium (wheat) in the horizontal direction (Table 5), K – lateral pressure quotient; calculated for wheat according to [10]: $K = 0.54 \cdot 1.11 = 0.60$.

In the analysis discrete computational model of the silo, the elastic constraints (boundary elements) model the bulk medium (wheat) without cohesion, meaning they cannot transmit tensile reactions. During numerical calculations using the ORCAN program, tensile boundary elements were eliminated by assuming a zero force value in the tensile boundary element. The computational procedure employed an iterative algorithm using the Newton–Raphson method.

3.2. Effects of thermal actions in the walls of silo battery

The effects of coupling static and thermal loads during the winter period in a battery of four wheat chambers are presented based on the analysis of thermal stresses and bending moments induced by the temperature gradient and the increases in latitudinal forces in the

reinforced concrete silo wall. Figure 6 shows the distribution of averaged thermal stresses in the wall around the perimeter of chambers K-1 and K-2 at a height of 4.5 m from the bottom. In the sunny zone in chamber K-1, loaded with a variable temperature field (points E and F), thermal stresses are twice as high as in the wall of chamber K-2. In both chambers, an increase in latitudinal stresses is visible near the monolithic contact.
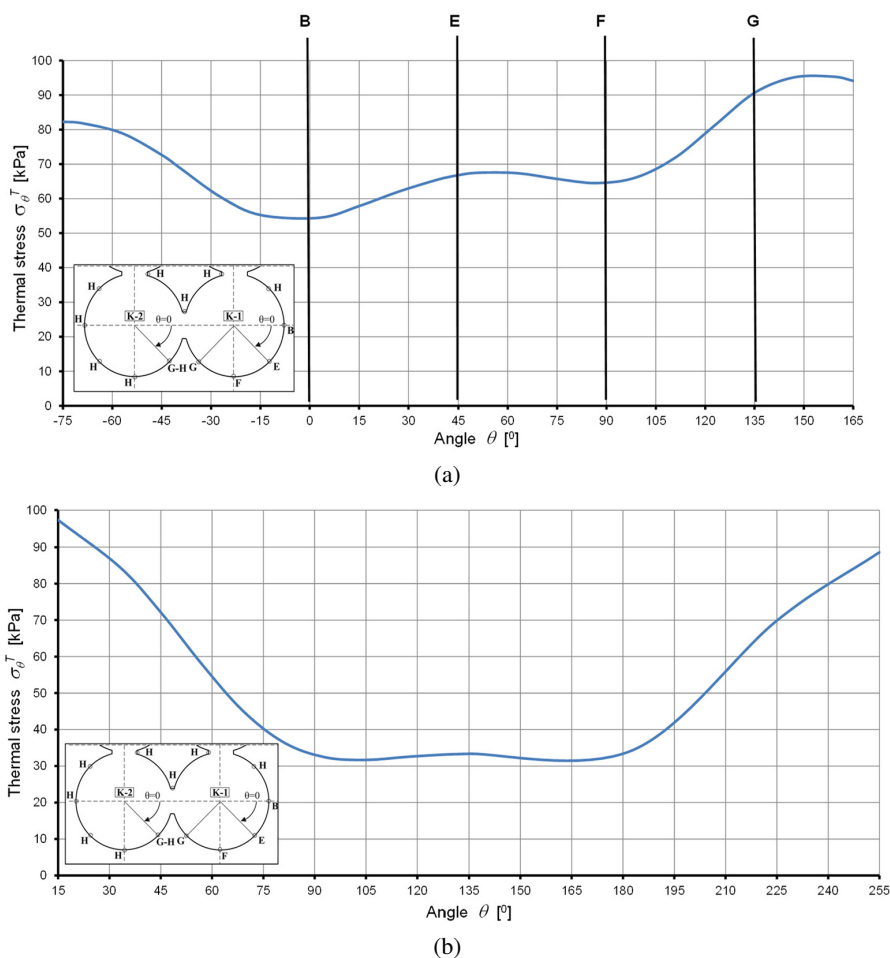

Fig. 6. Latitudinal stresses from thermal effects in the walls of the grain silo battery chambers: (a) Chamber K-1, (b) Chamber K-2

The stress state of the silos as a result of the coupling of the pressure of the granular medium (wheat) and the thermal impact from daily ambient temperature drops was determined in the form of increases in latitudinal forces in the silo wall from the thermal load N_θ^T in relation to the latitudinal force N_θ^J from Janssen's pressure (Table 6). In the sunny chamber K-1, the increases ranged from 7.6% to 12.7%, while in chambers K-2, K-3, and K-4, located in the

shade zone, these increases were smaller, ranging from 4.5% to 10.1%. The latitudinal forces N_θ^T were calculated on the basis of thermal stresses (Fig. 6). In both chambers K-1 and K-2, higher values of latitudinal forces from thermal stresses occurred in the wall cross-sections near the contact than in the area beyond the contact. In chamber K-1 the maximum differences in the values of forces N_θ^T near the contact and beyond the contact are about 70%, and in chamber K-2 located in the shadow zone of forces N_θ^T near the contact with chamber K-1 (angle $\theta = 15°$) are three times greater than in the cross-sections beyond the contact.

Table 6. Increases in latitudinal forces in the silo battery wall at the height of the chambers 4.5 m from the bottom caused by additional thermal impact

Chamber no.	Cross-sections beyond the junction of the chambers					Cross-sections at the junction of the chambers	
K-1 Chamber	$\theta = 3°$	$\theta = 45°$	$\theta = 87°$	$\theta = 135°$	$\theta = 315°$	$\theta = 165°$	$\theta = 285°$
N_θ^T [kN/m]	10.9	13.36	12.9	18.13	14.53	18.82	16.45
N_θ^J [kN/m]	143.20	143.20	143.20	143.20	143.20	133.36	133.36
N_θ^T/N_θ^J [%]	7.6	9.3	9.0	12.7	10.2	14.1	12.3
K-2 Chamber	$\theta = 45°$	$\theta = 93°$	$\theta = 135°$	$\theta = 183°$	$\theta = 225°$	$\theta = 15°$	$\theta = 255°$
N_θ^T [kN/m]	14.44	6.49	6.67	6.89	13.98	19.49	17.72
N_θ^J [kN/m]	143.20	143.20	143.20	143.20	143.20	133.36	133.36
N_θ^T/N_θ^J [%]	10.1	4.5	4.7	4.8	9.8	14.6	13.3
K-3 Chamber	$\theta = 135°$	$\theta = 177°$	$\theta = 225°$	$\theta = 267°$	$\theta = 315°$	$\theta = 105°$	$\theta = 345°$
N_θ^T [kN/m]	13.92	7.20	7.26	6.99	14.06	17.36	17.67
N_θ^J [kN/m]	143.20	143.20	143.20	143.20	143.20	133.36	133.36
N_θ^T/N_θ^J [%]	9.7	5.0	5.1	4.9	9.8	13.0	13.3
K-4 Chamber	$\theta = 45°$	$\theta = 225°$	$\theta = 267°$	$\theta = 315°$	$\theta = 357°$	$\theta = 75°$	$\theta = 195°$
N_θ^T [kN/m]	13.89	14.04	7.07	6.91	6.53	18.44	17.71
N_θ^J [kN/m]	143.20	143.20	143.20	143.20	143.20	133.36	133.36
N_θ^T/N_θ^J [%]	9.7	9.8	4.9	4.8	4.6	13.8	13.3

In chamber K-1 located in the zone of strong insolation (angle $\theta = 75°$), the latitudinal moments are 3.5 times greater than the bending moments in chamber K-2 covered by the shadow zone (Fig. 7). In chamber K-2, in the entire area beyond the contact, the latitudinal moments reach the maximum value of $M_\theta^T = 2.87$ kNm/m, while in the cross-sections just before the contact, the bending moment increases by about 45%.
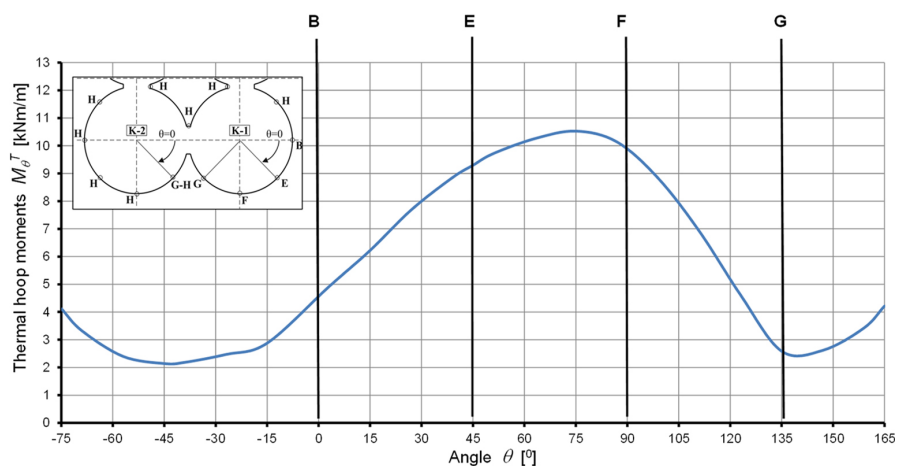
(a)
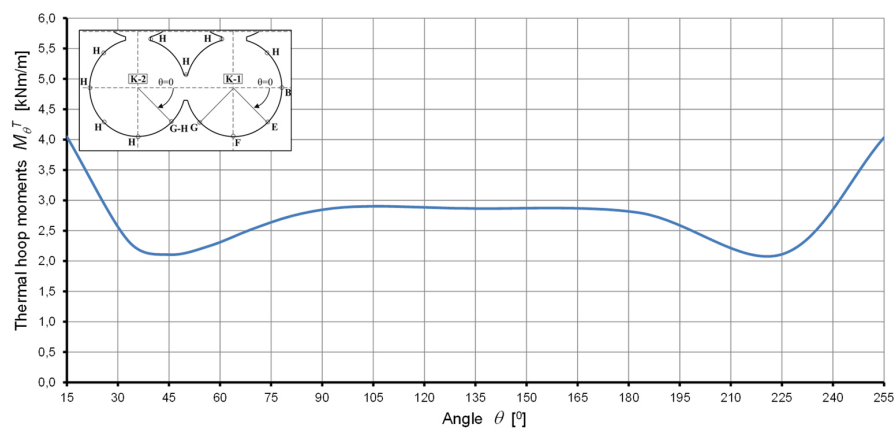
(b)

Fig. 7. Latitudinal moments in the walls of chambers K-1 (a) and K-2 (b) caused by the temperature gradient

4. Conclusions

Grain silo structures in operation are subjected to cyclically varying ambient temperature fields combined with static loads from the bulk medium and dynamic loads resulting from the silos' operation. Significant daily drops in ambient temperature, especially during winter and spring, coupled with grain pressure, can cause overloading of the reinforced concrete wall structures of grain silos. When analyzing the stress state of silo walls under the influence of thermal effects, the interaction between the silo wall structure and the bulk medium must be considered. Correctly determining the modulus of elasticity of grain stored in the silo is crucial. As a result of these drops in ambient temperature, additional tensile stresses (thermal stresses)

combined with bending develop in the wall cross-sections over a short period of time, resulting in increased cracking of the reinforced concrete walls of grain silos. The numerical analyses of the grain silos battery loaded with a non-stationary temperature field in winter confirmed the increase in latitudinal tensile stresses in the reinforced concrete wall, especially in the zone of strong insolation of the chambers.

Excessive thermal stresses, combined with fatigue or corrosion of concrete and reinforcing steel occurring in silos, ultimately reduce the durability and safety of silo structures. Furthermore, increased silo cracking can worsen grain storage conditions (e.g., local grain moisture) and reduce grain quality.

To ensure the durability and safe operation of grain silo structures, it is essential to design them with a specific level of reliability and operate them in accordance with the conditions assumed in the design. Continuous monitoring of the structure's stress level, starting from the first silo load cycle during operation, allows for monitoring the technical condition of the facility and forecasting whether the design life and reliability level of the silo structure will be maintained.

References

[1] P. Martens, *Silo-Handbuch*. Wilhelm Ernst & Sohn. Berlin, 1988.

[2] S.S. Safarian S.S. and E.C. Harris, "Schadensursachen an Stahlbetonsilos in den USA", *Beton- und Stahlbetonbau*, vol. 86, no. 2, pp. 35–37, 1991, doi: 10.1002/best.199100090.

[3] L. Runkiewicz, "Analysis of hazards, failures and disasters of reinforced concrete tanks and silos", *Przegląd Budowlany*, no. 4, pp. 75–79, 2012 (in Polish).

[4] H. Bayat, M. Chalecki, A. Leśniewska, M. Maj, J. Rybak, and A. Ubysz, "The cyclic load effect on the elasticity and plasticity deformation of high-strength reinforced concrete elements", *Archives of Civil and Mechanical Engineering*, vol. 24, no. 2, art. no. 135, 2024, doi:10.1007/s43452-023-00855-9.

[5] A. Ramirez, J. Garcia-Toment, and A. Tascon, "Experimental determination of self-heating and selfignition risks associated with the dusts of agricultural materials commonly stored in silos", *Journal of Hazardous Materials*, vol. 175, no. 1-3, pp. 920–927, 2010, doi:10.1016/j.jhazmat.2009.10.096.

[6] PN-EN 1990:2004 Eurocode. Basis of structural design. PKN, 2004 (in Polish).

[7] L. Runkiewicz and P. Lewiński, "Diagnostics, reinforcement and monitoring of reinforced and prestressed concrete tanks for bulk materials and liquids", *Przegląd Budowlany*, no. 10, pp. 25–32, 2014 (in Polish).

[8] L. Runkiewicz, *Principles of safety assessment and reinforcement of reinforced concrete silos. Instrukcje, Wytyczne, Poradniki ITB, no. 366*. Warszawa: Instytut Techniki Budowlanej, 2000 (in Polish).

[9] K. Kłos, G. Adamczewski, P. Woyciechowski, and P. Łukowski, "Carbonation of concrete cover of reinforcement as a cause of loss of durability of structures", *Archives of Civil Engineering*, vol. 69, no. 1, pp. 119–129, 2023, doi: 10.24425/ace.2023.144163.

[10] PN-EN 1991-4:2008 Eurocode 1. Actions on structures. Part 4: Silos and tanks. PKN, 2008 (in Polish).

[11] M. Maj and A. Ubysz, *Computational models for determining silo wall displacements caused by dry friction*. Oficyna Wydawnicza Politechniki Wrocławskiej, 2020.

[12] F. Askifi, H. Hammadeh, A. Ubysz, and M. Maj, "Numerical modeling of wall pressure in silo with and without insert", *Studia Geotechnica et Mechanica*, 2021, vol. 43, no. 1, pp. 22–33, 2021, doi: 10.2478/sgem-2020-0009.

[13] P. Anderson, Temperature stresses in steel grain-storage tanks. *Civil Engineering – ASCE*, vol. 36, no. 1, 1966.

[14] O.F. Theimer, Bersten von Stahlsilos bei tiefen Temperaturen. *Der Bauingenieur*, vol. 42, no. 3, pp. 102–105, 1967.

[15] A. Łapko, J. Kołłątaj, M. Gnatowski, J.A. Prusiel, R. Sokołowski, W. Konopacki, and J. Malesza, *Application of radio telemetry to the monitoring and testing of silo structures. Final Report on the Research Project. (Grant No 8 T07E 002 21)*. Politechnika Białostocka, 2003 (in Polish).

[16] El H. Bartali and F.J. Hatfield, "Forces in cylindrical grain silos caused by decreasing ambient temperature", *ACI Structural Journal*, vol. 87, no. 1, pp. 108–116, 1990.

[17] G.E. Blight, "Measurements on full size silos, Part 1: Temperature and strains", *Bulk Solids Handling*, vol. 7, no. 6, pp. 157–162, 1987.

[18] G.E. Blight, "Temperature-induced loading on silo walls", *Structural Engineering Review*, vol. 4, no. 1, pp. 61–71, 1992.

[19] A. Łapko and R. Tribiłło, "Influence of interaction of the bulk medium and silo bin on distribution of internal forces in circular wall cross sections", *Archives of Civil Engineering*, vol. 35, no. 3-4, pp. 313–327, 1989.

[20] K. Diamoutene and M. Kaminski, "Investigation of temperature and strain distribution in reinforced-concrete wall of a rapeseed storage silo", *Structural Concrete*, vol. 4, no. 3, pp. 109–116, 2003, doi: 10.1680/STCO.2003.4.3.109.

[21] A. Łapko and J.A. Prusiel, *Studies on thermal actions and forces in cylindrical storage silo bins. Handbook of Convening and handling of Particulate Solids*. Amsterdam: Elsevier, 2001, pp. 189–197.

[22] A. Łapko, M. Gnatowski, and J.A. Prusiel, "Analysis of some effects caused by interaction between bulk solid and r.c. silo wall structure", *Powder Technology*, vol. 133, no 1-3, pp. 44–53, 2003, doi: 10.1016/S0032-5910(03)00095-0.

[23] PN-B-03262:2002 Reinforced concrete silos for bulk materials. Static calculations, design, construction, and operation. PKN, 2002 (in Polish).

[24] A. Halicka and D.J. Franczak-Balmas, *Reinforced concrete tanks for liquids and bulk materials. Contemporary design principles with examples*. Warszawa: PWN, 2020 (in Polish).

[25] A. Łapko and J.A. Prusiel, "Analysis of thermal effects in grouped silos of grain elevators", *International Agrophysics*, vol. 20, no. 4, pp. 301–307, 2006.

[26] W.M.A. Khalifa and K.F.O. El-Kashif, "Computational Model for the Evaluation of Reinforced Concrete Silos Subjected to Thermal Load", *Engineering, Technology & Applied Science Research*, vol. 9, no. 4, pp. 4411–4418, 2019, doi: 10.48084/ETASR.2874.

[27] Z. Mohammad, M. Anwar, S.S Ansari, and A. Baqi, "Finite Element Modelling of RC Silo subjected to Thermal Loads", in *Recent Trends in Civil Engineering*. LNCE, vol. 274. Springer, 2023, pp. 419–427, doi: 10.1007/978-981-19-4055-2_33.

[28] A. Łapko and J. Kołłątaj, "The wireless technique of examination of silo wall structures during operation" in *Proceedings of the 4th International Conference for Conveying and Handling of Particulate Solids*, vol. 1. Budapest, Hungary, 2003, pp. 6.77–6.82.

[29] J.A. Prusiel, *Effects of coupled thermal, humidity and static interactions in reinforced concrete cylindrical grain silos*. Rozprawy Naukowe no. 271, Biblioteka Budownictwa, Oficyna Wydawnicza Politechniki Białostockiej, 2015 (in Polish).

[30] D. Gawin, *Modeling of coupled thermal and hygroscopic phenomena in building materials and elements*. Zeszyty Naukowe, no. 853, Rozprawy Naukowe, no. 279. Wydawnictwo Politechniki Łódzkiej, 2000 (in Polish).

[31] H. Garbalińska, *Isothermal moisture transport coefficients of porous building materials*. Prace Naukowe Politechniki Szczecińskiej, no. 571. Szczecin, 2002 (in Polish).

[32] A. Marynowicz and J. Wyrwał, *Testing selected moisture properties of building materials under isothermal conditions*. PAN KILiW, IPPT, Studia z zakresu Inżynierii, no. 52. Warszawa, 2005 (in Polish).

[33] T. Chyży, M. Mackiewicz, and S. Matulewicz, *Modern graphical language for describing building structures ORCAN version 0.91. Syntax and applications*. Oficyna Wydawnicza Politechniki Białostockiej, 2014 (in Polish).

[34] H.A. Janssen, "Versuche uber Getreidedruck in Silozellen. Zeitschrift", *Deutscher Ingenieure*, vol. 39, pp. 1045–1049, 1895.

[35] H.B. Manbeck and G.L. Nelson, "Three dimensional constitutive equations for wheat en masse", *Transactions of the ASAE*, vol. 18, no. 6, pp. 1122–1127, 1975.

Stan wytężenia żelbetowych ścian baterii silosów na zboże poddanych oddziaływaniom statycznym i termicznym – badania in situ i analiza numeryczna

Streszczenie:

W eksploatowanych żelbetowych silosach na zboże występują stany awaryjne (np. zwiększone zarysowanie żelbetowych ścian), których przyczyną mogą być stany przeciążenia konstrukcji komór związane z gwałtownym spadkiem temperatury otoczenia w ciągu doby. Dobowe spadki temperatury otoczenia wywołują naprężenia termiczne w powłoce silosu. Występowanie dodatkowych naprężeń termicznych w silosie spowodowane jest interakcją ściany i ośrodka sypkiego składowanego w silosie. Efektem tego jest wystąpienie w przekrojach ściany komory silosu dodatkowych naprężeń rozciągających połączonych ze zginaniem. W pracy przedstawiono wyniki badań *in situ* w okresie wczesnozimowym rozkładów pól temperatury na elewatorze zbożowym w Podlaskich Zakładach Zbożowych w Białymstoku. Do badań na obiekcie wykorzystano specjalistyczny prototypowy system telemetryczny SensoNet umożliwiający ciągły monitoring eksploatowanych baterii silosów i rejestrację wielkości fizycznych, takich jak: odkształcenia i temperatura. Pomierzone zmienne pola temperatur na powierzchni komór silosowych posłużyły do wyznaczenia metodą różnic skończonych nieliniowych rozkładów temperatury na grubości żelbetowych ścian w baterii silosów na zboże. Przeprowadzono metodą elementów skończonych obliczenia numeryczne czterech silosów zblokowanych na zboże poddanych oddziaływaniom statycznym (parcie *Janssena* materiału sypkiego) i termicznym. Na podstawie analizy wyników obliczeń numerycznych (MES) przedstawiono niekorzystne efekty sprzężenia obciążeń termicznych i statycznych w postaci przyrostów rozciągających naprężeń równoleżnikowych i momentów zginających w żelbetowych ścianach baterii silosów na zboże.